Pol. J. Environ. Stud. Vol. XX, No. X (XXXX), 1-17
DOI: 10.15244/pjoes/241483 ONLINE PUBLICATION DATE: 2026-11-20

Original Research

From Pollution Load to Economic Output: Matching Fertilizer-Related Non-Point Source Pollution with Agricultural Economic Performance across Chinese Provinces

Zhiyi Xu*

School of Public Administration, Jiangsu Open University, Nanjing 210036, Jiangsu, China

Received: 01 July 2026
Accepted: 06 October 2026

Abstract

Fertilizer-related non-point source pollution remains a major constraint on agricultural green development. This study estimated provincial fertilizer-related non-point source pollution loads in China from 2015 to 2024 using the official coefficient-based accounting framework, covering TN, TP, and NH_3-N. Pollution load intensity was further constructed by dividing total pollution load by agricultural economic output. Based on average agricultural GDP, provinces were classified into high, medium, and low agricultural-economic regions using the tertile method. Dagum Gini decomposition, global and local Moran's I, and the Spatial Durbin Model were employed to examine regional inequality, spatial clustering, and driving mechanisms. Results show that total fertilizer-related pollution load declined from 8.91×10^5 t in 2015 to 5.80×10^5 t in 2024, while average load intensity decreased by 63.10%. Regional inequality remained relatively high, with inter-regional net inequality as the main source. Significant positive spatial autocorrelation was observed, with high–high clusters mainly in southeastern and south-central provinces. The SDM results indicate that operational scale and infrastructure reduced load intensity, whereas fiscal support intensity and technological conditions showed positive local associations. Spatial spillovers were mainly linked to planting structure, operational scale, and technological conditions. These findings support differentiated and coordinated governance of agricultural non-point source pollution.

Keywords: fertilizer-related non-point source pollution, pollution load intensity, spatial Durbin model

*e-mail: xuzhiyi@slaas.cn
0009-0000-2307-4932

© 2026 This article is licensed under a Creative Commons Attribution-NonCommercial 4.0 International (CC BY-NC 4.0)

Introduction

Fertilizer inputs underpin agricultural intensification and food security, but excessive or inefficient use increases nitrogen and phosphorus losses to the environment [1]. Optimized nutrient management can reduce cropland nitrogen pollution without sacrificing productivity [2]. China is especially relevant because of its large agricultural sector and long-term reliance on chemical fertilizers [3]. Fertilizer use has changed markedly across space and time, remains regionally uneven, and continues to pose environmental risks, although nitrogen-use efficiency has improved under recent reduction and efficiency policies [4].

Agricultural non-point source pollution is diffuse, delayed, and spatially heterogeneous [5], with nutrients transported through runoff, leaching, erosion, and irrigation return flow [6]. Losses also depend on rainfall, soils, hydrology, and land use [7]. Existing research has examined policy, land tenure, subsidy reform, fertilizer behavior, total emissions, fertilizer intensity, and broad pollution indices, but less attention has been paid to pollution pressure per unit of agricultural economic output [8]. A key issue in this field is how fertilizer-related non-point source pollution load is measured. Many existing studies estimate agricultural pollution using inventory methods, emission coefficient methods, or export coefficient models [9, 10]. These approaches are useful because they are relatively simple, data-accessible, and suitable for regional comparison. However, they often rely on fixed coefficients or aggregate fertilizer input indicators, which may not fully distinguish between crop-sowing processes and garden-land production, nor do they always account for provincial differences in pollutant loss coefficients and annual changes in fertilizer application intensity. The export coefficient model, for instance, remains widely used for estimating agricultural non-point source pollution because of its simplicity, but recent methodological work also notes that such models need improvement when pollutant transport and regional heterogeneity are considered [11].

This study therefore applies China's official coefficient-based framework for planting-sector water pollutants. It distinguishes crop-sown and garden land, uses provincial loss coefficients for TN, TP, and NH_3-N, and adjusts TN/NH_3-N and TP loads by nitrogen- and phosphate-fertilizer intensity, respectively. The resulting measure captures fertilizer-related nutrient-loss pressure while accounting for land-use type, provincial coefficients, and annual fertilizer intensity.

Pollution load intensity complements absolute load by relating environmental pressure to agricultural economic output [12]. Evaluating fertilizer-related performance therefore requires considering input reduction, nutrient-use efficiency, and economic output together [13]. Regional heterogeneity is another important issue. Existing studies often divide China into eastern, central, western, and northeastern regions [14]. In addition, agricultural systems are spatially connected through production patterns, factor mobility, technology diffusion, infrastructure, and environmental linkages; ignoring such dependence can bias estimates of pollution drivers [15].

Against this background, this study estimates fertilizer-related non-point source pollution loads for 31 Chinese provinces from 2015 to 2024, covering TN, TP, and NH_3-N. It then constructs fertilizer-related non-point source pollution load intensity by dividing total pollution load by agricultural economic output. Based on average agricultural GDP during 2015-2024, the provinces are classified into high, medium, and low agricultural-economic regions using the tertile method. Dagum Gini decomposition is used to identify the sources of regional inequality, global and local Moran's I are applied to examine spatial clustering, and the Spatial Durbin Model is used to investigate local drivers and spatial spillover effects.

The study contributes by combining an official coefficient-based pollution accounting framework with an output-based intensity measure and an agricultural-economic regional classification, then integrating inequality decomposition, spatial autocorrelation, and spatial econometric analysis. This framework provides evidence for differentiated and coordinated agricultural non-point source pollution governance.

Materials and Methods

Study Area and Data Sources

This study focuses on 31 provincial-level administrative regions in mainland China from 2015 to 2024. Hong Kong, Macao, and Taiwan were excluded because of differences in statistical systems and data availability. The dataset covers fertilizer use, cropland and orchard-related land use, agricultural economic output, agricultural production conditions, fiscal expenditure, agricultural disaster exposure, and agricultural employment.

The fertilizer data include the converted amounts of nitrogen fertilizer, phosphate fertilizer, and potash fertilizer. Land-use and production data include total sown area of crops, sown area of grain crops, garden land area, effective irrigated area, and crop disaster-affected area. Economic and input-related data include the added value of the primary industry, total power of agricultural machinery, expenditure on agriculture, forestry, and water affairs, and employment in the primary industry.

To ensure comparability across provinces and years, all raw data were standardized before analysis. Area variables were converted into hectares or thousand hectares, pollution loads were converted into tons, and economic output variables were converted into 100 million yuan. For a small number of missing observations, linear interpolation or trend

extrapolation was used according to adjacent-year changes. The final dataset is a balanced provincial panel consisting of 31 provinces over 10 years, with 310 observations.

Accounting of Fertilizer-Related Non-Point Source Pollution Loads

Pollution loads are estimated using the Ministry of Ecology and Environment's official planting-sector coefficient framework. It covers TN, TP, and NH_3-N losses from crop and garden land associated with rainfall, irrigation, runoff, and leaching.

Fertilizer-related non-point source pollution loads are calculated as follows:

$$Q_{j,it} = (A_{g,it}e_{gj,i} + A_{y,it}e_{yj,i}) \times \frac{q_{j,it}}{q_{j,i,2017}} \times 10^{-3}$$

where $Q_{j,it}$ denotes pollution load of pollutant j in province i in year t, measured in tons; j represents TN, TP, or NH_3-N; $A_{g,it}$ is the total sown area of crops in province i in year t, measured in hm^2; $A_{y,it}$ is the garden land area, measured in hm^2; $e_{gj,i}$ is the loss coefficient of pollutant j from the crop-sowing process in province i, measured in kg/hm^2; $e_{yj,i}$ is the loss coefficient of pollutant j from garden land in province i, measured in kg/hm^2; $q_{j,it}$ denotes the fertilizer application intensity per unit area in the survey year; $q_{j,i,2017}$ denotes the fertilizer application intensity per unit area in 2017; and 10^{-3} is the unit conversion coefficient from kilograms to tons.

For TN and NH_3-N, the correction factor is based on nitrogen fertilizer application intensity per unit area. For TP, the correction factor is based on phosphate fertilizer application intensity per unit area. Specifically:

$$q_{N,it} = \frac{N_{it}}{A_{g,it} + A_{y,it}}, q_{P,it} = \frac{P_{it}}{A_{g,it} + A_{y,it}}$$

where $q_{N,it}$ denotes nitrogen fertilizer application intensity per unit area in province i in year t; $q_{P,it}$ denotes phosphate fertilizer application intensity per unit area; N_{it} and P_{it} denote the converted amounts of nitrogen fertilizer and phosphate fertilizer, respectively. Since potash fertilizer is not included in the official accounting scope of planting-sector water pollutants, it is not directly included in the calculation of TN, TP, or NH_3-N loads.

The total fertilizer-related non-point source pollution loads in province i in year t are then calculated as:

$$Q_{it} = Q_{TN,it} + Q_{TP,it} + Q_{NH_3-N,it}$$

where Q_{it} denotes the total fertilizer-related non-point source pollution loads, measured in tons.

Construction of Fertilizer-Related Non-Point Source Pollution Load Intensity

Pollution loads reflect the absolute scale of environmental pressure, but they cannot fully capture the pollution burden associated with each unit of agricultural economic output. Therefore, this study constructs fertilizer-related non-point source pollution load intensity to measure the environmental pressure embedded in agricultural economic output:

$$I_{it} = \frac{Q_{it}}{AGDP_{it}}$$

where I_{it} denotes fertilizer-related non-point source pollution load intensity in province i in year t, measured in tons per 100 million yuan; Q_{it} denotes total fertilizer-related non-point source pollution loads; and $AGDP_{it}$ denotes agricultural economic output. Due to data availability, the added value of the primary industry is used as a proxy for agricultural economic output. A higher value of I_{it} indicates greater fertilizer-related non-point source pollution pressure per unit of agricultural economic output, whereas a lower value indicates a relatively greener agricultural production process.

For terminological consistency, this study uses "pollution load" to denote the absolute estimated quantity of TN, TP, and NH_3-N, and "pollution load intensity" to denote total pollution load per unit of agricultural economic output. The term "fertilizer-related non-point source pollution" is used as the general description of the environmental phenomenon, whereas pollution load intensity is the dependent variable used in the spatial econometric analysis.

To reduce heteroscedasticity and the influence of extreme values, the natural logarithm of pollution load intensity is used in the spatial econometric model:

$$\ln I_{it} = \ln\left(\frac{Q_{it}}{AGDP_{it}}\right)$$

In addition, to test the robustness of the benchmark results, this study constructs three pollutant-specific load intensity indicators:

$$\ln I_{it} = \rho W \ln I_{it} + X_{it}\beta + WX_{it}\theta + \mu_i + \lambda_t + \varepsilon_{it}$$

Among these indicators, the natural logarithm of TN load intensity is used as the alternative dependent variable in the reported robustness check.

Measurement of Regional Inequality: Dagum Gini Coefficient and Its Decomposition

To examine regional differences in fertilizer-related non-point source pollution load intensity and identify their sources, this study adopts the Dagum Gini

coefficient and its decomposition method. Compared with the traditional Gini coefficient, the Dagum Gini coefficient not only measures the overall level of inequality but also decomposes total inequality into intra-regional inequality, inter-regional net inequality, and transvariation density [16]. This makes it possible to identify whether regional disparities mainly arise from differences within the same agricultural economic group, systematic gaps between different groups, or overlapping distributions across groups.

The overall Gini coefficient is calculated as follows:

$$G = \frac{\sum_{j=1}^{k}\sum_{h=1}^{k}\sum_{i=1}^{n_j}\sum_{r=1}^{n_h} | y_{ji} - y_{hr} |}{2n^2\bar{y}}$$

Where G denotes the overall Gini coefficient; k is the number of regions; n_j and n_h are the numbers of provinces in regions j and h, respectively; y_{ji} and y_{hr} represent the fertilizer-related non-point source pollution load intensity of province i in region j and province r in region h, respectively; n is the total number of provinces; and $\bar{y}$ is the mean fertilizer-related non-point source pollution load intensity of all provinces.

According to the Dagum decomposition framework, the overall Gini coefficient can be decomposed as follows:

$$G = G_w + G_{nb} + G_t$$

where G_w denotes the contribution of intra-regional inequality, reflecting differences in fertilizer-related non-point source pollution load intensity among provinces within the same region; G_{nb} denotes the contribution of inter-regional net inequality, reflecting the effect of average differences between different regions on overall inequality; and G_t denotes the contribution of transvariation density, reflecting inequality caused by distributional overlap across regions.

A larger intra-regional contribution indicates that disparities in pollution load intensity are mainly generated by heterogeneity among provinces within the same agricultural economic group. A larger inter-regional net contribution suggests a more pronounced systematic gap between regions with different agricultural GDP levels. A larger transvariation density contribution indicates stronger distributional overlap among regions; in other words, some provinces in the low-agricultural-GDP group may have higher pollution load intensity than those in the medium- or high-agricultural-GDP groups, or some provinces in the high-agricultural-GDP group may have lower pollution load intensity than provinces in other groups.

These three components are additive contributions to the overall Gini coefficient. Their magnitudes are compared to identify the dominant source of inequality.

In this study, the 31 provinces are divided into high-GDP, medium-GDP, and low-GDP groups according to the tertile classification based on their average agricultural GDP from 2015 to 2024. Based on this classification, the Dagum Gini coefficient and its decomposition results are calculated using the SPSSAU platform (www.spssau.com), and the results are used to identify the sources of inequality in fertilizer-related non-point source pollution load intensity across regions with different agricultural economic scales.

Spatial Autocorrelation Analysis

Fertilizer-related non-point source pollution load intensity may exhibit spatial dependence. On the one hand, neighboring provinces often share similar agricultural natural conditions, cropping systems, fertilizer application patterns, and farmland management practices. On the other hand, agricultural non-point source pollution may be spatially connected through watershed systems, topography, and regional agricultural production linkages. Therefore, this study uses global Moran's I and local Moran's I to examine the spatial autocorrelation of fertilizer-related non-point source pollution load intensity [17].

Global Moran's I is used to test whether pollution load intensity exhibits overall spatial clustering. It is calculated as:

$$I = \frac{n}{S_0}\frac{\sum_{i=1}^{n}\sum_{j=1}^{n} w_{ij}\,(x_i - \bar{x})(x_j - \bar{x})}{\sum_{i=1}^{n}(x_i - \bar{x})^2}$$

where I denotes global Moran's I; n is the number of provinces; x_i and x_j denote the pollution load intensity of provinces i and j, respectively; $\bar{x}$ is the sample mean; w_{ij} is the element of the spatial weight matrix; and $S_0 = \sum_i \sum_j w_{ij}$. A significantly positive Moran's I indicates positive spatial autocorrelation, meaning that high-intensity provinces tend to be adjacent to other high-intensity provinces, while low-intensity provinces tend to be adjacent to other low-intensity provinces. A significantly negative Moran's I indicates spatial dispersion.

Local Moran's I is used to identify local spatial association patterns for each province. It is calculated as:

$$I_i = (x_i - \bar{x})\sum_{j=1}^{n} w_{ij}\,(x_j - \bar{x})$$

Based on the local spatial association results, provinces can be classified into four types: high–high, low–low, high–low, and low–high. The high–high type indicates that both a province and its neighboring provinces have high pollution load intensity; the low–low type indicates that both a province and its neighboring provinces have low pollution load intensity; and the high–low and low–high types indicate local spatial heterogeneity.

Spatial Weight Matrix

The spatal weight matrix is the basis for spatial autocorrelation analysis and spatial econometric modeling. This study uses a contiguity spatial weight matrix as the benchmark matrix. If two provinces share a common border, $w_{ij} = 1$; otherwise, $w_{ij} = 0$. The diagonal elements are set to zero, namely $w_{ii} = 0$, and the matrix is row-standardized.

The contiguity matrix captures spatial linkages caused by geographical adjacency, similar agricultural production conditions, regional policy interactions, and potential cross-boundary environmental connections. It is therefore suitable as the benchmark spatial weight matrix for provincial-level agricultural non-point source pollution analysis.

For the spatial autocorrelation analysis, this study additionally employs an economic–geographic nested matrix. This matrix jointly considers geographical proximity and economic similarity and is used to examine whether the overall spatial association remains robust under a broader definition of interprovincial spatial linkage.

Spatial Durbin Model

If significant spatial autocorrelation exists in fertilizer-related non-point source pollution load intensity, conventional panel models may produce biased estimates by ignoring spatial dependence. Therefore, this study constructs a Spatial Durbin Model to examine both local effects and spatial spillover effects of influencing factors on fertilizer-related non-point source pollution load intensity [18].

The model is specified as follows:

$$\ln I_{it} = \rho W \ln I_{it} + X_{it}\beta + WX_{it}\theta + \mu_i + \lambda_t + \varepsilon_{it}$$

where $\ln I_{it}$ denotes the natural logarithm of fertilizer-related non-point source pollution load intensity in province i in year t; $W\ln I_{it}$ is the spatially lagged dependent variable; ρ is the spatial autoregressive coefficient, measuring the influence of neighboring provinces' pollution load intensity on local pollution load intensity; X_{it} is the matrix of explanatory variables; β represents the coefficients of local explanatory variables; WX_{it} represents the spatially lagged explanatory variables; θ captures the effects of neighboring provinces' explanatory variables on local pollution load intensity; μ_i denotes province fixed effects; λ_t denotes year fixed effects; and ε_{it} is the random error term. For consistency, W×X denotes the spatially lagged explanatory variable X, while W×ln pollution load intensity denotes the spatially lagged dependent variable.

This study considers six categories of influencing factors: planting structure, production technology, farmland infrastructure, fiscal support, natural risk, and operational scale. The explanatory variables include the share of grain crop sown area, the share of garden land, agricultural mechanization intensity, effective irrigation rate, fiscal expenditure intensity for agriculture, forestry, and water affairs, crop disaster rate, and agricultural operational scale.

The variables are constructed as follows:

$$Grain_{it} = \frac{Grain\ crop\ sown\ area_{it}}{Total\ crop\ sown\ area_{it}}$$

$$Garden_{it} = \frac{Garden\ land\ area_{it}}{Total\ crop\ sown\ area_{it}}$$

$$Mach_{it} = \frac{Total\ power\ of\ agricultural\ machinery_{it}}{Total\ crop\ sown\ area_{it}}$$

$$Irrig_{it} = \frac{Effective\ irrigated\ area_{it}}{Total\ crop\ sown\ area_{it}}$$

$$Fiscal_{it} = \frac{Expenditure\ on\ agriculture,\ forestry,\ and\ water\ affairs_{it}}{Added\ value\ of\ the\ primary\ industry_{it}}$$

$$Disaster_{it} = \frac{Crop\ disaster\text{-}affected\ area_{it}}{Total\ crop\ sown\ area_{it}}$$

$$Scale_{it} = \frac{Total\ crop\ sown\ area_{it}}{Employment\ in\ the\ primary\ industry_{it}}$$

The share of grain crop sown area reflects regional grain production structure. The share of garden land represents the planting structure of perennial cash crops. Agricultural mechanization intensity reflects the level of agricultural production technology and equipment. The effective irrigation rate measures farmland infrastructure conditions. Fiscal expenditure intensity reflects government support for agriculture-related development and environmental governance. The crop disaster rate captures natural risk and production uncertainty. Agricultural operational scale measures the sown area per agricultural worker and reflects the scale of agricultural operation.

Their selection reflects channels that may alter fertilizer demand, application efficiency, nutrient uptake and loss, technology adoption, disaster response, and standardized nutrient management. Together they represent the main production, technological, infrastructural, institutional, natural, and organizational conditions associated with provincial pollution-load intensity.

To reduce dimensional differences and the influence of extreme values, this study takes the natural logarithm of pollution load intensity, agricultural mechanization intensity, fiscal expenditure intensity, and agricultural operational scale.

Effect Decomposition and Robustness Checks

Because the Spatial Durbin Model includes both the spatially lagged dependent variable and the spatially lagged explanatory variables, the estimated coefficients cannot be directly interpreted as conventional marginal effects. Therefore, this study further decomposes the SDM results into direct effects, indirect effects, and total effects.

The direct effect reflects the impact of a local explanatory variable on local fertilizer-related non-point source pollution load intensity. The indirect effect reflects the spatial spillover effect transmitted to neighboring provinces. The total effect is the sum of the direct and indirect effects.

To test the reliability of the empirical results, this study conducts two robustness checks. First, Beijing, Tianjin, Shanghai, and Chongqing are excluded from the sample, and the Spatial Durbin Model is re-estimated to reduce the potential influence of municipalities with distinctive administrative scales, agricultural structures, and production conditions. Second, the dependent variable is replaced with TN load intensity, and the model is re-estimated to examine whether the signs and significance of the main results remain stable under an alternative measure of fertilizer-related pollution pressure.

Through the above methodological framework, this study systematically examines the spatiotemporal evolution, regional inequality, spatial dependence, and driving mechanisms of fertilizer-related non-point source pollution load intensity across Chinese provinces.

Regional Classification

Provinces are ranked by average agricultural GDP during 2015-2024 and divided by tertiles into high-, medium-, and low-GDP groups, allowing inequality to be examined by agricultural economic scale rather than conventional geography.

The high-GDP group includes Henan, Shandong, Sichuan, Jiangsu, Heilongjiang, Guangdong, Hubei, Hebei, Hunan, and Guangxi. The medium-GDP group includes Xinjiang, Yunnan, Shaanxi, Guizhou, Anhui, Liaoning, Inner Mongolia, Fujian, Jiangxi, and Zhejiang. The low-GDP group includes Chongqing, Gansu, Jilin, Shanxi, Hainan, Ningxia, Tianjin, Qinghai, Shanghai, Beijing, and Tibet.

Based on this classification, the subsequent regional inequality analysis takes the high-GDP, medium-GDP, and low-GDP groups as the basic analytical units. This grouping highlights the differentiation of pollution load intensity under different agricultural economic scales and helps determine whether inequality in fertilizer-related non-point source pollution load intensity is mainly driven by systematic differences among regions with different agricultural GDP levels or by heterogeneity within the same agricultural economic group.

Results

Changes in Fertilizer-Related Non-Point Source Pollution Load

Fig. 1 summarizes these temporal changes and shows that the decline occurred across all three agricultural-economic regions, while the absolute pollution load remained concentrated in the high agricultural-economic region. From 2015 to 2024, the TN, TP, and NH_3-N loads in the three agricultural-economic regions all showed a downward trend. The total load of the three pollutants decreased from 8.91×10^5 t in 2015 to 5.80×10^5 t in 2024, a reduction of 3.11×10^5 t, corresponding to a decline of 34.93%. Specifically, the total load in the high agricultural-economic region decreased from 5.42×10^5 t to 3.72×10^5 t, that in the medium agricultural-economic region decreased from 3.05×10^5 t to 1.78×10^5 t, and that in the low agricultural-economic region decreased from 0.44×10^5 t to 0.29×10^5 t.

National TN load declined by 34.56%, from 7.28×10^5 t to 4.76×10^5 t. In 2024, high-, medium-, and low-GDP

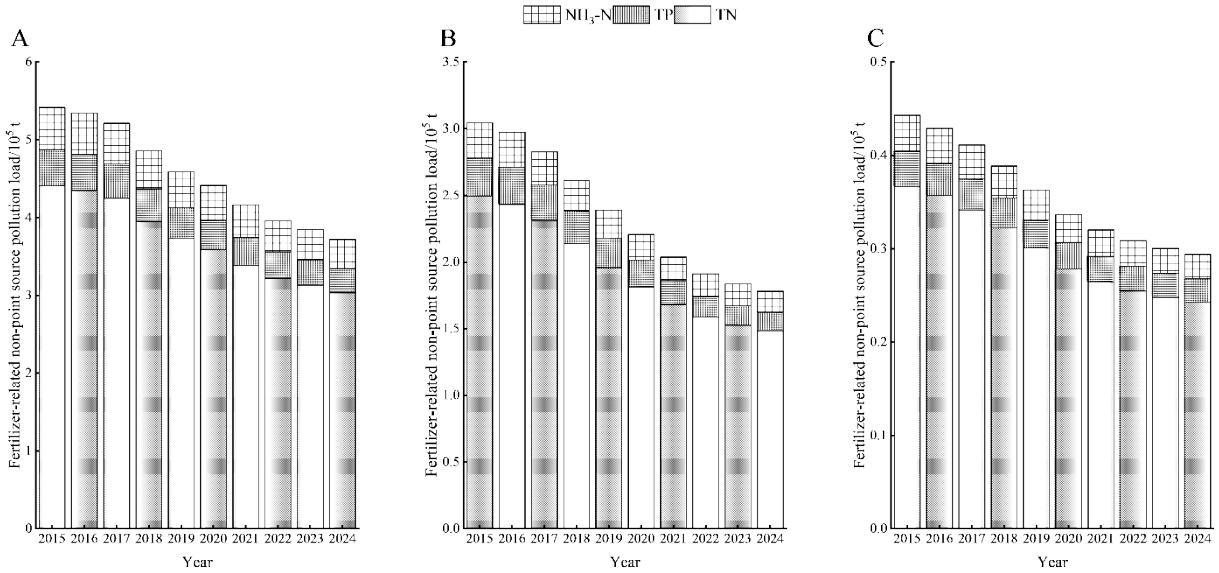


Fig. 1. Changes in fertilizer-related non-point source pollution loads across agricultural-economic regions in China, 2015-2024.

groups accounted for 63.73%, 31.18%, and 5.09% of TN load, respectively.

For TP load, the high agricultural-economic region decreased from 0.46×10^5 t in 2015 to 0.31×10^5 t in 2024, a reduction of 0.15×10^5 t, or 32.40%. The medium agricultural-economic region decreased from 0.28×10^5 t to 0.14×10^5 t, a reduction of 0.14×10^5 t, or 50.63%. The low agricultural-economic region decreased from 0.04×10^5 t to 0.03×10^5 t, a reduction of 0.01×10^5 t, or 33.92%. Overall, the TP load decreased from 0.78×10^5 t to 0.48×10^5 t, with a decline of 39.09%. In 2024, the high, medium, and low agricultural-economic regions accounted for 65.32%, 29.39%, and 5.29% of the total TP load, respectively.

For NH_3-N load, the high agricultural-economic region decreased from 0.54×10^5 t in 2015 to 0.37×10^5 t in 2024, a reduction of 0.17×10^5 t, or 31.14%. The medium agricultural-economic region decreased from 0.27×10^5 t to 0.16×10^5 t, a reduction of 0.11×10^5 t, or 41.08%. The low agricultural-economic region decreased from 0.04×10^5 t to 0.03×10^5 t, a reduction of 0.01×10^5 t, or 31.57%. Overall, the NH_3-N load decreased from 0.85×10^5 t to 0.56×10^5 t, with a decline of 34.29%. In 2024, the high, medium, and low agricultural-economic regions accounted for 67.06%, 28.23%, and 4.71% of the total NH_3-N load, respectively.

Changes in Fertilizer-Related Non-Point Source Pollution Load Intensity

Fig. 2 shows a broad decline in pollution load intensity alongside persistent interprovincial differences. The national average fell from 14.83 to 5.47 t/100 million yuan between 2015 and 2024, a 63.10% reduction. Regional averages also declined: high-, medium-, and low-GDP groups fell from 19.63 to 7.65, 18.85 to 6.58, and 6.83 to 2.49 t/100 million yuan, respectively. The high-GDP group remained highest and the low-GDP group lowest throughout.

At the provincial level, in 2015, the provinces with relatively high fertilizer-related non-point source pollution load intensity were Guangxi, Jiangxi, Zhejiang, Hunan, and Guangdong, with values of 47.75 t/100 million yuan, 42.57 t/100 million yuan, 34.72 t/100 million yuan, 32.36 t/100 million yuan, and 31.05 t/100 million yuan, respectively. In 2024, the provinces with relatively high load intensity were still mainly Guangxi, Jiangxi, Guangdong, Anhui, and Zhejiang, with values of 19.13 t/100 million yuan, 16.98 t/100 million yuan, 12.50 t/100 million yuan, 11.73 t/100 million yuan, and 10.05 t/100 million yuan, respectively.

For low-intensity provinces, in 2015, Tibet, Inner Mongolia, Xinjiang, Ningxia, and Qinghai recorded

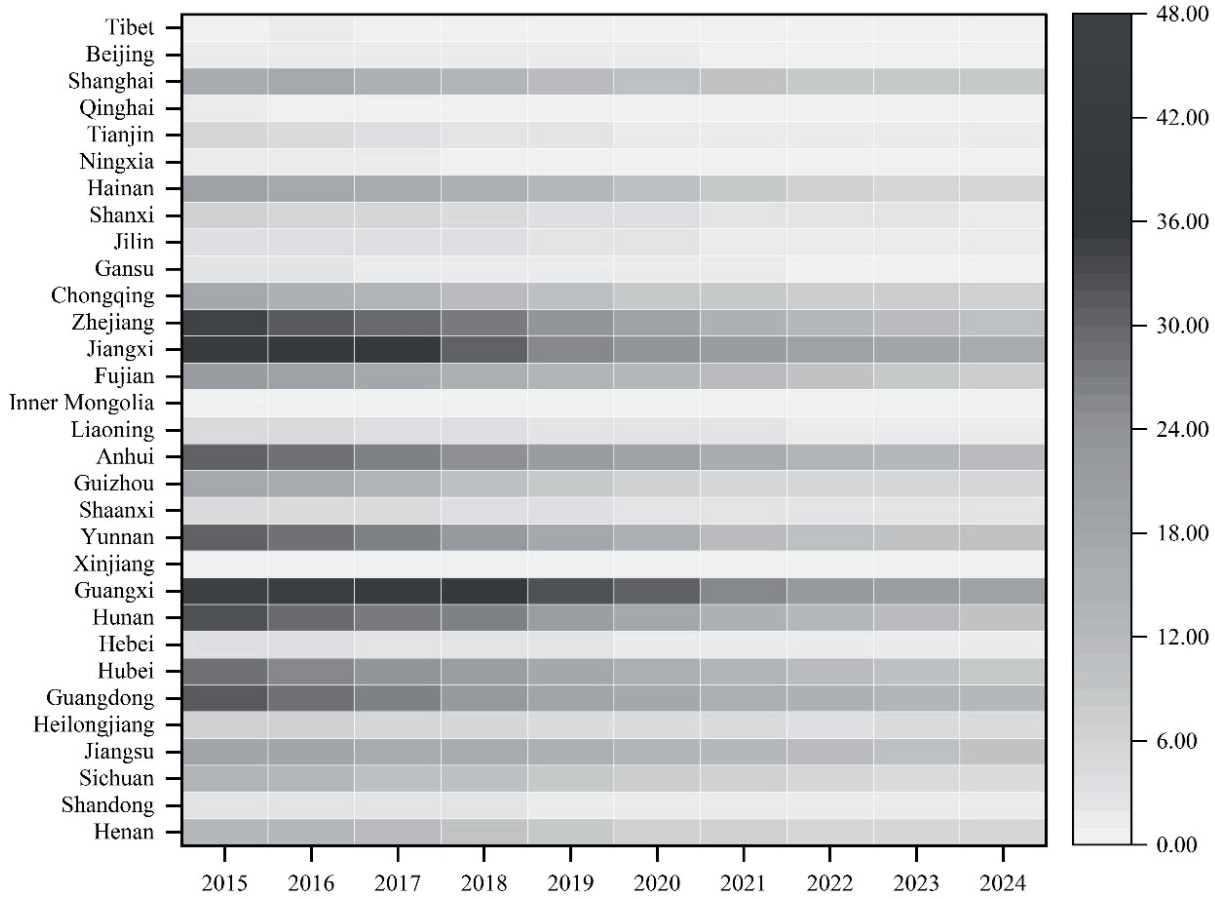


Fig. 2. Spatiotemporal changes in fertilizer-related non-point source pollution load intensity across Chinese provinces, 2015-2024.

the lowest load intensity values, at 0.87 t/100 million yuan, 0.94 t/100 million yuan, 0.98 t/100 million yuan, 1.06 t/100 million yuan, and 1.20 t/100 million yuan, respectively. In 2024, the provinces with the lowest load intensity were Tibet, Qinghai, Inner Mongolia, Xinjiang, and Ningxia, with values of 0.17 t/100 million yuan, 0.28 t/100 million yuan, 0.36 t/100 million yuan, 0.48 t/100 million yuan, and 0.51 t/100 million yuan, respectively.

In terms of absolute reduction, the provinces with the largest decreases from 2015 to 2024 were Guangxi, Jiangxi, Zhejiang, Hunan, and Yunnan, with reductions of 28.61 t/100 million yuan, 25.59 t/100 million yuan, 24.66 t/100 million yuan, 22.64 t/100 million yuan, and 21.37 t/100 million yuan, respectively. In terms of relative reduction, Tibet, Qinghai, Hainan, Tianjin, and Guizhou showed the largest declines, at 80.22%, 76.18%, 74.32%, 72.95%, and 71.72%, respectively. Overall, fertilizer-related non-point source pollution load intensity declined widely across provinces from 2015 to 2024, although clear interprovincial differences remained.

Regional Inequality in Fertilizer-Related Non-Point Source Pollution Load Intensity

From 2015 to 2024, the overall Gini coefficient of fertilizer-related non-point source pollution load intensity remained between 0.50 and 0.51, showing only minor fluctuations. Specifically, the overall Gini coefficient was 0.50 from 2015 to 2017, increased to 0.51 in 2018, declined to 0.50 in 2019, remained at 0.51 from 2020 to 2023, and fell again to 0.50 in 2024. This indicates that provincial disparities in fertilizer-related non-point source pollution load intensity remained relatively high but stable during the study period.

According to the Dagum decomposition results, the intra-regional inequality contribution G_w remained stable at 0.14 throughout 2015-2024, indicating that disparities among provinces within the same agricultural-economic region were largely unchanged. The inter-regional net inequality contribution G_{nb} increased from 0.20 in 2015 to 0.22 during 2021-2023, before decreasing slightly to 0.21 in 2024. The transvariation density contribution G_t decreased from 0.16 in 2015 to 0.14 in 2024, suggesting that the distributional overlap among different agricultural-economic regions weakened to some extent.

Inter-regional net inequality was consistently the largest component, identifying between-group differences as the dominant source of overall inequality. Within groups, the low-GDP region had the greatest inequality (Gini 0.53 to 0.56), followed by the medium-GDP region (0.44 to 0.45), whereas the high-GDP region declined from 0.40 to 0.38 (Table 1).

Global Spatial Autocorrelation of Fertilizer-Related Non-Point Source Pollution Load Intensity

Table 2 reports the annual Moran's I statistics under both spatial weight matrices, highlighting the persistence but gradual weakening of positive spatial autocorrelation. From 2015 to 2024, the global Moran's I values of fertilizer-related non-point source pollution load intensity were all positive and statistically significant under both spatial weight matrices. Under the contiguity matrix, Moran's I decreased from 0.69 in 2015 to 0.62 in 2024, with all p-values <0.001. The corresponding z-values remained high, decreasing from 6.10 to 5.52. This indicates that fertilizer-related non-point source pollution load intensity exhibited significant positive spatial autocorrelation throughout the study period.

Table 1. Dagum Gini coefficient and decomposition results of fertilizer-related non-point source pollution load intensity.

Year	Gini coefficient				Internal Gini coefficient		
	Overall	G_w	G_{nb}	G_t	High agricultural-economic region	Medium agricultural-economic region	Low agricultural-economic region
2015	0.50	0.14	0.20	0.16	0.40	0.44	0.53
2016	0.50	0.14	0.20	0.16	0.39	0.43	0.51
2017	0.50	0.14	0.20	0.16	0.40	0.44	0.53
2018	0.51	0.14	0.20	0.16	0.40	0.44	0.54
2019	0.50	0.14	0.20	0.16	0.39	0.44	0.53
2020	0.51	0.14	0.21	0.16	0.40	0.45	0.54
2021	0.51	0.14	0.22	0.15	0.39	0.45	0.54
2022	0.51	0.14	0.22	0.15	0.39	0.45	0.55
2023	0.51	0.14	0.22	0.15	0.39	0.45	0.56
2024	0.50	0.14	0.21	0.14	0.38	0.45	0.56

Note: G_w,, $G_{nb,}$ and G_t denote the intra-regional inequality contribution, inter-regional net inequality contribution, and transvariation-density contribution, respectively.

Table 2. Global Moran's I of fertilizer-related non-point source pollution load intensity.

Year	Moran's I under contiguity matrix	z-value	p-value	Moran's I under economic–geographic nested matrix	z-value	p-value
2015	0.69	6.10	<0.001	0.22	7.31	<0.001
2016	0.69	6.07	<0.001	0.22	7.31	<0.001
2017	0.68	6.03	<0.001	0.22	7.29	<0.001
2018	0.66	5.89	<0.001	0.22	7.25	<0.001
2019	0.66	5.85	<0.001	0.22	7.29	<0.001
2020	0.65	5.75	<0.001	0.21	7.14	<0.001
2021	0.65	5.73	<0.001	0.21	7.08	<0.001
2022	0.63	5.63	<0.001	0.20	6.89	<0.001
2023	0.63	5.61	<0.001	0.20	6.87	<0.001
2024	0.62	5.52	<0.001	0.20	6.79	<0.001

Under the economic-geographic nested matrix, Moran's I values were lower than those under the contiguity matrix but remained consistently positive and significant. The index remained at 0.22 from 2015 to 2019, decreased to 0.21 in 2020 and 2021, and further declined to 0.20 from 2022 to 2024. The z-values ranged from 6.79 to 7.31, and all p-values were <0.001, confirming that the positive spatial correlation remained robust after considering both geographic proximity and economic linkage.

Overall, the results show that fertilizer-related non-point source pollution load intensity had a clear spatial clustering pattern during 2015-2024. Provinces with high load intensity tended to be spatially adjacent to or associated with other high-intensity provinces, while provinces with low load intensity tended to be associated with other low-intensity provinces. The gradual decline in Moran's I under both matrices suggests that the degree of spatial clustering weakened slightly over time, although the spatial dependence remained statistically significant.

The decline in Moran's I indicates moderate weakening, not disappearance, of spatial dependence. It may reflect convergence in fertilizer management, technology diffusion, infrastructure improvement, and widespread fertilizer-reduction policies; these are plausible mechanisms rather than causal effects identified by Moran's I.

Local Spatial Autocorrelation Characteristics

Fig. 3 visualizes the local spatial association patterns for 2015, 2020, and 2024, illustrating the persistence of the main high–high and low–low clusters and the local transition observed in Guizhou. To further identify the local spatial clustering pattern of fertilizer-related non-point source pollution load intensity, this study selected 2015, 2020, and 2024 for local Moran's I analysis. The results show that the local spatial association patterns were mainly characterized by high–high clustering and low–low clustering, indicating relatively stable local spatial differentiation across provinces.

In 2015, significant low–low clustering was mainly observed in Hebei, Shanxi, Inner Mongolia, Liaoning, Jilin, Gansu, Qinghai, Ningxia, and Xinjiang. Among them, Inner Mongolia, Hebei, Gansu, Ningxia, and Xinjiang had relatively high local Moran's I values, at 0.79, 0.61, 0.71, 0.87, and 0.97, respectively. Significant high–high clustering was mainly found in Zhejiang, Anhui, Fujian, Jiangxi, Hubei, Hunan, Guangdong, Guangxi, and Guizhou. Among these provinces, Jiangxi, Hunan, Guangdong, and Guangxi recorded relatively high local Moran's I values, at 2.15, 1.46, 1.52, and 2.25, respectively. Shanghai also showed a high–high clustering pattern, although its significance was at a marginal level.

By 2020, the main low–low and high–high clusters remained broadly unchanged, while Guizhou shifted from high–high to significant low–high clustering (local Moran's I = −0.17).

In 2024, the local spatial clustering pattern remained highly stable. Low–low clustering was mainly observed in Hebei, Shanxi, Inner Mongolia, Liaoning, Gansu, Qinghai, Ningxia, and Xinjiang, with local Moran's I values of 0.59, 0.43, 0.71, 0.59, 0.72, 0.78, 0.82, and 0.95, respectively. High–high clustering was mainly found in Shanghai, Zhejiang, Anhui, Fujian, Jiangxi, Hubei, Hunan, Guangdong, and Guangxi. Among them, Jiangxi, Guangdong, and Guangxi recorded relatively high local Moran's I values, at 2.02, 1.68, and 1.88, respectively. Guizhou continued to show significant low–high clustering, with a local Moran's I value of −0.07.

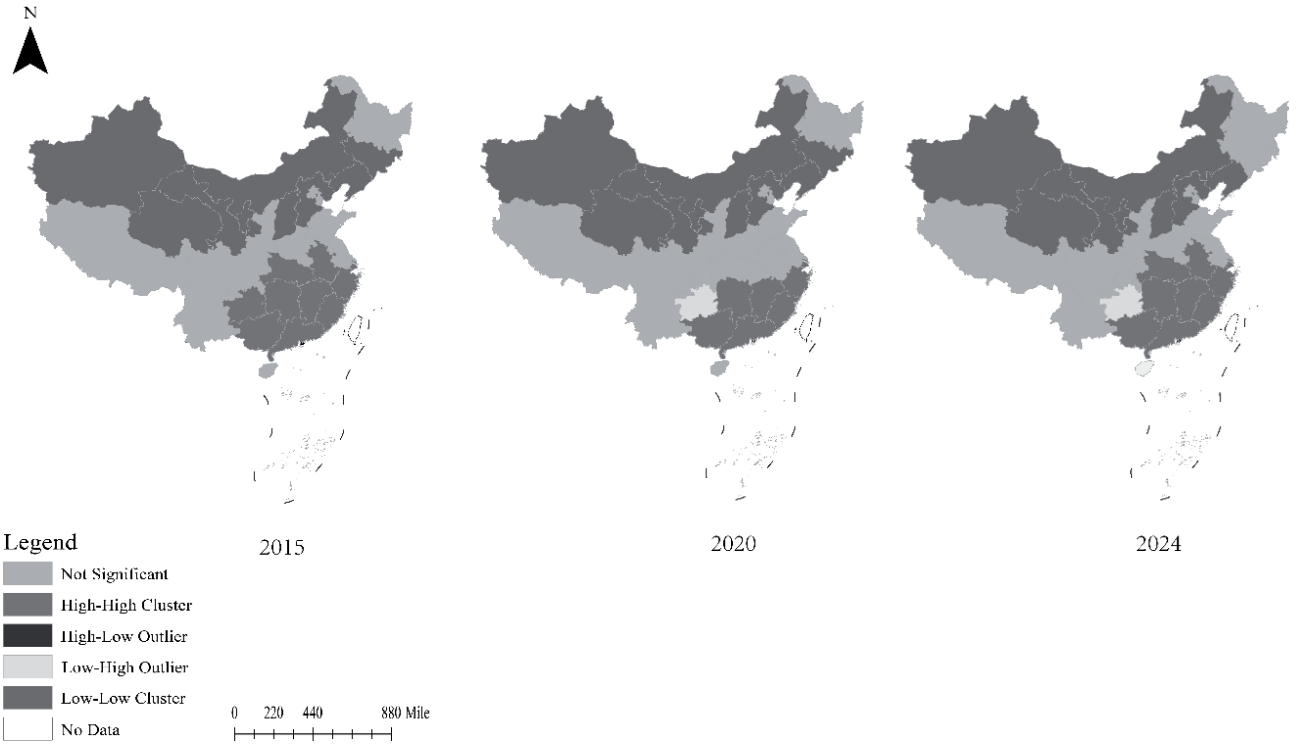


Fig. 3. Local spatial association patterns of fertilizer-related non-point source pollution load intensity in China, 2015, 2020, and 2024.

Spatial Durbin Model Estimation Results and Spatial Effect Decomposition

The Spatial Durbin Model results show that the spatial autoregressive coefficient (ρ) is 0.48 and significant at the 1% level, indicating persistent positive spatial dependence in fertilizer-related non-point source pollution load intensity. Because the SDM contains both the spatially lagged dependent variable and spatially lagged explanatory variables, the raw coefficients cannot be interpreted directly as marginal effects. Therefore, the substantive interpretation focuses on the decomposed direct, indirect, and total effects reported in Table 3.

Planting structure has no significant direct effect (−0.08), but its indirect effect is significantly positive (2.89, $p<0.01$), resulting in a positive total effect (2.81, $p<0.05$). This suggests that the association between planting structure and pollution load intensity is transmitted mainly through cross-regional spatial linkages rather than through the local channel. By contrast, cash crop structure shows no statistically significant direct, indirect, or total effect.

Fiscal support intensity exhibits a significantly positive direct effect (0.29, $p<0.01$) and total effect (0.36, $p<0.01$), while its indirect effect is not statistically significant. This indicates that the positive association of fiscal expenditure intensity on agriculture, forestry, and water affairs with pollution load intensity is mainly local. Operational scale shows significant negative direct (−0.20, $p<0.05$), indirect (−0.65, $p<0.01$), and total effects (−0.85, $p<0.01$), indicating that larger-scale agricultural operation is associated with lower pollution load intensity both locally and through spatial linkages.

Technological conditions display a significantly positive direct effect (0.29, $p<0.01$) but a significantly negative indirect effect (−0.39, $p<0.01$). The total effect is negative but statistically insignificant (−0.10), suggesting that the positive local association of mechanization with pollution load intensity is largely offset by a negative cross-regional association. Infrastructure has a significantly negative direct effect (−0.72, $p<0.01$) and total effect (−0.95, $p<0.05$), whereas its indirect effect is not significant. Natural risk shows no significant direct, indirect, or total effect. Overall, the effect decomposition reveals heterogeneous local and spatial channels that are not fully captured by the raw SDM coefficients alone.

The raw SDM parameter estimates and the corresponding direct, indirect, and total effects are reported together in Table 3. This combined presentation distinguishes the estimated coefficients of the local and spatially lagged explanatory variables from the marginal effects derived from the spatial effect decomposition.

Robustness Checks

To test the reliability of the benchmark Spatial Durbin Model results, two robustness checks were conducted. First, Beijing, Tianjin, Shanghai, and Chongqing were excluded from the sample, and the model was re-estimated to reduce the potential influence of municipalities with distinctive administrative scales,

Table 3. Spatial Durbin Model estimation results and spatial effect decomposition for fertilizer-related non-point source pollution load intensity.

Variable	Coef.	W×X	Direct effect	Indirect effect	Total effect
Planting structure	-0.10	2.84**	-0.08	2.89**	2.81*
Cash crop structure	-0.95	0.10	-0.95	0.08	-0.87
Fiscal support intensity	0.29**	0.06	0.29**	0.07	0.36**
ln operational scale	-0.20*	-0.64**	-0.20*	-0.65**	-0.85**
Technological conditions	0.29**	-0.38**	0.29**	-0.39**	-0.10
Infrastructure	-0.72**	-0.21	-0.72**	-0.23	-0.95*
Natural risk	0.10	0.15	0.11	0.15	0.26
Spatial autoregressive coefficient (ρ)	0.48**	-	-	-	-

Note: Coef. and *W*×X report the raw SDM parameter estimates for local and spatially lagged explanatory variables, respectively; the direct, indirect, and total effects are obtained from the spatial effect decomposition. W denotes the row-standardized spatial weight matrix. N = 310; pseudo-R^2 = 0.91; spatial pseudo-R^2 = 0.90. * and ** indicate $p<0.05$ and $p<0.01$, respectively.

agricultural structures, and production conditions. Second, the dependent variable was replaced by TN load intensity, and the Spatial Durbin Model was re-estimated.

After excluding municipalities, the signs and significance levels of the main variables remained broadly consistent with the benchmark results. The coefficient of fiscal support intensity was 0.28, significant at the 1% level, while the coefficient of ln operational scale was −0.18, significant at the 5% level. Technological conditions had a significantly positive coefficient of 0.28. Among the spatially lagged variables, *W*×ln operational scale and *W*×Technological conditions were −1.03 and −0.70, respectively, both significant at the 1% level. The coefficient of the spatially lagged dependent variable was 0.30, also significant at the 1% level, indicating that fertilizer-related non-point source pollution load intensity still exhibited significant positive spatial dependence after excluding municipalities.

The results also remained stable after replacing the dependent variable with TN load intensity. Fiscal support intensity, ln operational scale, technological conditions, and infrastructure had coefficients of 0.30, −0.17, 0.29, and −0.66, respectively, all statistically significant and consistent in direction with the benchmark model. Among the spatially lagged variables, *W*×Planting structure, *W*×ln operational scale, and *W*×Technological conditions were 2.77, −0.63, and −0.38, respectively, all significant at the 1% level. The coefficient of the spatially lagged dependent variable was 0.49, indicating that TN load intensity also had significant positive spatial dependence (Table 4).

Heterogeneity Analysis

To further examine differences in the driving mechanisms of fertilizer-related non-point source pollution load intensity across agricultural-economic regions, this study estimates the Spatial Durbin Model separately for the high, medium, and low agricultural-economic regions. The results show clear heterogeneity in both local influencing factors and spatial dependence across the three regions.

In the high agricultural-economic region, planting structure, fiscal support intensity, and operational scale have significant effects on fertilizer-related non-point source pollution load intensity. The coefficient of planting structure is 6.68, significant at the 1% level. The coefficient of fiscal support intensity is 0.51, also significant at the 1% level. The coefficient of ln operational scale is −0.54, significant at the 1% level, indicating that the expansion of agricultural operational scale is associated with lower pollution load intensity. The coefficient of the spatially lagged dependent variable is 0.56, significant at the 1% level, suggesting strong positive spatial dependence within the high agricultural-economic region. However, the spatially lagged explanatory variables are not statistically significant, indicating that the effects of neighboring explanatory variables on local pollution load intensity are relatively limited in this region.

In the medium agricultural-economic region, fiscal support intensity and operational scale show significant local effects, with coefficients of 0.27 and −0.81, respectively. The spatially lagged explanatory variables exhibit stronger significance in this region. The coefficients of *W*×Planting structure, *W*×Cash crop structure, *W*×Fiscal support intensity, *W*×ln operational scale, and *W*×Infrastructure are 3.11, 3.75, 0.38, −0.43, and −0.96, respectively, all statistically significant. The coefficient of the spatially lagged dependent variable is 0.22, significant at the 5% level. These results indicate that fertilizer-related non-point source pollution load intensity in the medium agricultural-economic region is affected not only by local factors but also by neighboring provinces' agricultural structure, fiscal support intensity, operational scale, and infrastructure conditions.

Table 4. Robustness check results.

Variable	Excluding municipalities	Replacing dependent variable
Planting structure	-0.15	0.03
Cash crop structure	-1.40	-0.88
Fiscal support intensity	0.28**	0.30**
ln operational scale	-0.18*	-0.17*
Technological conditions	0.28**	0.29**
Infrastructure	-0.45	-0.66**
Natural risk	0.00	0.10
W×Planting structure	1.30	2.77**
W×Cash crop structure	-2.93	0.15
W×Fiscal support intensity	-0.05	0.05
W×ln Operational scale	-1.03**	-0.63**
W×Technological conditions	-0.70**	-0.38**
W×Infrastructure	0.37	-0.22
W×Natural risk	0.29	0.14
W×ln dependent variable	0.30**	0.49**
Observations	270	310
R^2	0.91	0.91

Note: In the model excluding municipalities, the dependent variable is the natural logarithm of fertilizer-related non-point source pollution load intensity. In the alternative dependent variable model, the dependent variable is the natural logarithm of TN load intensity. * and ** indicate significance at the 5% and 1% levels, respectively. *W* denotes the spatially lagged term.

In the low-GDP group, fiscal support was positive, operational scale and infrastructure were negative, and spatial lags of cash crop structure and operational scale were negative; the spatially lagged dependent variable was insignificant (Table 5).

Discussion

Declining Fertilizer-Related Non-Point Source Pollution Load and Implications for Agricultural Green Transition

The results show that fertilizer-related non-point source pollution load and load intensity both declined from 2015 to 2024. This indicates that China's agricultural production system has experienced a measurable reduction in fertilizer-related environmental pressure during the study period. The decline is consistent with recent evidence that China's agricultural non-point source pollution has entered a stage of policy-driven reduction, supported by fertilizer reduction policies, improved agricultural input management, and increasing attention to green agricultural development [14, 19]. Recent studies have also shown that agricultural non-point source pollution in China has gradually shifted from rapid growth to mitigation under stronger policy intervention and agricultural modernization [20].

TN remained the dominant pollutant, consistent with its sensitivity to fertilizer use, irrigation, rainfall, and runoff [21, 22]. Yet lower intensity did not eliminate absolute pressure: high-GDP regions still accounted for most TN, TP, and NH_3-N loads in 2024. Policy assessment should therefore distinguish absolute load from load intensity and consider agricultural structure and ecological sensitivity together [23].

Regional Inequality and the Meaning of Agricultural-Economic Regional Classification

This study classified provinces into high, medium, and low agricultural-economic regions according to their average agricultural GDP during 2015-2024. Compared with conventional geographical divisions, this classification better reflects the relationship between agricultural economic scale and fertilizer-related non-point source pollution load intensity. The results show that the high and medium agricultural-economic regions generally had higher load intensity than the low agricultural-economic region, but all three regions showed declining trends. This indicates that regions with larger agricultural economies tend to face higher fertilizer-related pollution pressure, but they

Table 5. Heterogeneity results of the spatial Durbin Model across agricultural-economic regions.

Variable	High agricultural-economic region	Medium agricultural-economic region	Low agricultural-economic region
Planting structure	6.68**	0.64	1.97
Cash crop structure	3.24	-2.10	-3.48
Fiscal support intensity	0.51**	0.27*	0.59**
ln operational scale	-0.54**	-0.81**	-1.40**
Technological conditions	0.03	0.09	0.22
Infrastructure	-0.99	-0.12	-2.59**
Natural risk	-0.09	-0.04	0.15
W×Planting structure	1.22	3.11*	-1.64
W×Cash crop structure	3.55	3.75*	-6.10**
W×Fiscal support intensity	-0.19	0.38**	0.13
W×ln operational scale	0.15	-0.43*	-1.19**
W×Technological conditions	-0.04	0.05	0.49
W×Infrastructure	0.23	-0.96*	-1.24
W×Natural risk	0.3	0.25	0.11
W×ln pollution load intensity	0.56**	0.22*	-0.08
Observations	100	100	110
R^2	0.93	0.92	0.87

Note: The dependent variable is the natural logarithm of fertilizer-related non-point source pollution load intensity. * and ** indicate significance at the 5% and 1% levels, respectively. *W* denotes the spatially lagged term.

may also have stronger capacity for input optimization, technological upgrading, and pollution load intensity reduction.

The Dagum Gini decomposition further shows that inter-regional net inequality was the main source of overall inequality in fertilizer-related non-point source pollution load intensity. This means that systematic differences among the high, medium, and low agricultural-economic regions played a larger role than within-region heterogeneity. This finding is consistent with recent research showing that agricultural non-point source pollution varies significantly across functional zones, production structures, and regional development levels [24, 25]. Studies on rural aging, agricultural structure, and non-point source pollution also show that the effect of agricultural production conditions differs across grain-producing areas, balanced production-consumption areas, and grain-consuming areas [24].

A notable result is that the low agricultural-economic region had the highest internal Gini coefficient. This suggests that the low agricultural-economic region is not homogeneous. It includes metropolitan municipalities with small agricultural sectors, such as Beijing, Shanghai, and Tianjin, as well as western and plateau provinces with strong natural constraints, such as Tibet, Qinghai, and Ningxia. Therefore, the internal disparity of the low agricultural-economic region may be driven by differences in agricultural function, land endowment, production structure, and the denominator effect of agricultural economic output. Similar arguments have been made in recent studies emphasizing that agricultural non-point source pollution is spatially heterogeneous and jointly affected by natural conditions, economic development, and agricultural production systems [19].

Spatial Clustering and the Need for Cross-Regional Governance

Global and local Moran's I show persistent spatial clustering, with high–high clusters concentrated mainly in southeastern and south-central provinces and low–low clusters in northern and northwestern provinces, consistent with prior spatial evidence on agricultural pollution and fertilizer intensity [26].

The significant positive coefficient of the spatially lagged dependent variable in the Spatial Durbin Model further confirms the existence of spatial dependence. In practical terms, this means that provinces with high fertilizer-related pollution load intensity tend to be spatially associated with higher pollution load intensity in neighboring or spatially connected provinces. This may occur through similar cropping systems, regional agricultural specialization, cross-boundary

watershed linkages, shared technology adoption patterns, and policy imitation among neighboring provinces. Recent studies on rural industrial integration and agricultural non-point source pollution also show that agricultural production changes can generate spatial spillover effects through factor mobility, technology diffusion, and regional interaction [27].

These findings imply that fertilizer-related non-point source pollution should not be managed only within administrative boundaries. In high–high clusters, especially in southeastern and south-central agricultural regions, cross-provincial coordination is necessary. Policy tools such as coordinated fertilizer reduction, regional nutrient management, watershed-based monitoring, and joint agricultural green technology extension may be more effective than isolated provincial interventions. This is consistent with recent proposals for zoning-based agricultural non-point source pollution management, which emphasize differentiated and coordinated governance across ecological and agricultural production zones [23].

Operational Scale, Infrastructure, and Pollution Load Intensity Reduction

Operational scale has negative direct, indirect, and total effects, suggesting both local and cross-regional reductions in pollution load intensity. Larger operations may more readily adopt mechanized fertilization, soil testing, socialized services, and standardized nutrient management [28]; related studies also link land transfer and productive services to lower fertilizer pollution or agrochemical intensity [14].

Scale expansion is not automatically beneficial: prior evidence shows that higher scale efficiency can coincide with greater pollution under some conditions [28]. Its environmental gains therefore depend on accompanying nutrient management and green technology. Infrastructure mainly reduces local pollution intensity, plausibly through better water-fertilizer coordination and nutrient uptake; nutrient losses also depend on precipitation, runoff, irrigation, land use, and hydrology [22].

Interpreting the Positive Fiscal-Support Association and the Contrasting Technological Effects

Fiscal support intensity has positive direct and total effects but no significant indirect effect. Because the proxy covers agriculture, forestry, and water affairs, it mixes production support, infrastructure, disaster prevention, irrigation, and environmental spending; the positive association may therefore reflect heavier production tasks or pollution-control pressure rather than an adverse effect of regulation itself [29].

Technological conditions exhibit a significantly positive direct effect but a significantly negative indirect effect, while the total effect is not statistically significant. The positive direct effect may reflect the fact that agricultural mechanization is often associated with more intensive production, larger input use, and stronger agricultural specialization, so mechanization can coincide with higher local production intensity and pollution load intensity. In contrast, the negative indirect effect may reflect demonstration effects, agricultural service spillovers, and technology diffusion from neighboring provinces. The insignificant total effect indicates that these opposing local and spatial associations largely offset each other.

This dual effect is consistent with recent research on fertilizer use efficiency and spatial spillovers. Studies have shown that fertilizer use efficiency in China still has room for improvement and depends on technological innovation, institutional change, and production-service systems. Other spatial studies also indicate that fertilizer application intensity has spatial spillover effects, and that mechanization and agricultural modernization may affect fertilizer reduction differently across regions and production systems [30].

Heterogeneous Mechanisms across Agricultural-Economic Regions

The heterogeneity analysis shows that the driving mechanisms differ across the three agricultural-economic regions. In the high agricultural-economic region, planting structure, fiscal support intensity, operational scale, and the spatially lagged dependent variable were significant. This suggests that fertilizer-related pollution load intensity in agriculturally developed regions is mainly shaped by local agricultural production structure and strong spatial dependence. Since these regions bear the largest absolute pollution loads, policy should focus on precision fertilization, nutrient balance management, and interprovincial coordination in major agricultural production areas.

In the medium agricultural-economic region, spatially lagged explanatory variables were more active. Planting structure, cash crop structure, fiscal support intensity, operational scale, and infrastructure in neighboring provinces all showed significant spatial effects. This indicates that the medium agricultural-economic region is more sensitive to external regional influences. Its pollution load intensity is affected not only by local agricultural conditions but also by neighboring provinces' production structure, policy input, and infrastructure. Similar spatial spillover mechanisms have been reported in recent studies on rural three-industry integration, fertilizer use intensity, and agricultural green development [31].

In the low agricultural-economic region, operational scale and infrastructure had strong negative effects, while the spatially lagged dependent variable was not significant. This suggests that local production conditions are more important than spatial dependence in this region. The low agricultural-economic region contains both metropolitan areas with small agricultural sectors and western regions with ecological or natural

constraints. Therefore, differentiated policies are needed. Metropolitan provinces should emphasize high-value, low-pollution, and precision-managed agriculture, while western and plateau provinces should focus on improving farmland infrastructure, moderate-scale operation, and ecological constraint-based input efficiency.

Policy Implications

The results provide several policy implications. First, high agricultural-economic regions should remain the priority areas for absolute pollution load reduction. Although their load intensity declined, their TN, TP, and NH_3-N loads remained high. These regions need stricter nutrient budgeting, precision fertilization, manure substitution, and runoff control in major grain and cash crop production systems.

Second, cross-regional governance should be strengthened in high–high clusters. Since fertilizer-related pollution load intensity shows significant spatial dependence, pollution reduction in one province may be affected by neighboring provinces. Joint monitoring, watershed-based governance, regional agricultural service platforms, and coordinated fertilizer reduction policies should be promoted.

Third, operational scale should be combined with green production services. The negative effect of operational scale suggests that scale management can reduce pollution load intensity, but only when accompanied by technology services, standardized fertilization, and environmental constraints. Recent studies on farmland transfer, agricultural productive services, and fertilizer efficiency support this integrated policy direction [14].

Fourth, fiscal expenditure indicators should be refined. The positive coefficient of fiscal support intensity suggests that broad expenditure on agriculture, forestry, and water affairs may combine production support, infrastructure investment, ecological governance, and other policy functions. Future policy evaluation should therefore distinguish among production support, infrastructure investment, ecological compensation, fertilizer-reduction subsidies, and direct pollution-control spending. Recent studies on subsidy reform and fertilizer non-point source pollution also suggest that different subsidy designs may have different environmental effects [32].

Limitations and Future Research

This study has several limitations. First, due to data availability, the added value of the primary industry was used as a proxy for agricultural economic output. Since this indicator includes forestry, animal husbandry, and fisheries, it may dilute or amplify fertilizer-related pollution load intensity in some provinces. Future research should use planting-sector value added, crop output value, or crop-specific economic output when consistent data become available.

Second, this study used an official coefficient-based accounting method to estimate provincial fertilizer-related non-point source pollution loads. This approach is suitable for macro-level panel analysis, but it cannot fully capture natural processes such as rainfall intensity, slope, soil texture, drainage, and watershed connectivity. Process-based models such as InVEST and other hydrological or nutrient export models can complement coefficient-based accounting and improve the interpretation of pollutant migration mechanisms [33].

Third, this study used provinces as the spatial unit. Provincial data are useful for identifying macro-scale patterns and policy differences, but they cannot reveal county-level, watershed-level, or household-level mechanisms. Recent micro-level studies show that farmland transfer, household aging, subsidy policy, off-farm employment, mechanization adoption, and crop type can all affect fertilizer behavior and non-point source pollution. Future research should combine provincial spatial econometric analysis with county-level panels, watershed monitoring, and household survey data [24].

Overall, this study contributes to the literature by linking official pollution load accounting with agricultural economic output and by examining fertilizer-related non-point source pollution load intensity across agricultural-economic regions. The findings show that China's fertilizer-related pollution pressure has declined, but regional inequality and spatial dependence remain significant. Future studies should further extend this framework to crop-specific systems, watershed processes, and micro-level farmer behavior to support more precise and differentiated agricultural non-point source pollution governance.

Conclusions

This study estimates provincial fertilizer-related TN, TP, and NH_3-N loads for 2015–2024 and links them to agricultural economic output. Total load fell from 8.91×10^5 to 5.80×10^5 t, while load intensity declined substantially.

Regional inequality remained high, driven mainly by inter-regional differences, and the low-GDP group showed the greatest internal heterogeneity. Spatial clustering was persistently positive. SDM results indicate that operational scale and infrastructure are associated with lower load intensity, while fiscal support and technological conditions exhibit more complex local and spatial patterns.

Overall, fertilizer-related non-point source pollution governance in China should combine load reduction, intensity control, regional differentiation, and cross-regional coordination. High agricultural-economic regions should remain priority areas for absolute load reduction, while low agricultural-economic regions should focus on infrastructure improvement and scale-based management.

AI Usage Disclosure Statement

During the preparation of this work, the author used OpenAI ChatGPT-5.6 Sol in order to assist in English language editing, grammatical correction, and manuscript polishing. After using these tools, the author reviewed and edited the content as needed and takes full responsibility for the content of the published article.

Conflict of Interest

The author declares no conflict of interest.

References

1. LI C., ALUKO O.O., YUAN G., LI J., LIU H. The responses of soil organic carbon and total nitrogen to chemical nitrogen fertilizers reduction base on a meta-analysis. Scientific Reports, **12** (1), 16326, **2022**.
2. GU B., ZHANG X., LAM S.K., YU Y., VAN GRINSVEN H.J.M., ZHANG S., WANG X., BODIRSKY B. L., WANG S., DUAN J., REN C., BOUWMAN L., DE VRIES W., XU J., SUTTON M.A., CHEN D. Cost-effective mitigation of nitrogen pollution from global croplands. Nature, **613** (7942), 77, **2023**.
3. JI Y., LIU H., SHI Y. Will China's fertilizer use continue to decline? Evidence from LMDI analysis based on crops, regions and fertilizer types. PLoS ONE, **15** (8), e0237234, **2020**.
4. HAO L., SHUQIN L., YUFEI Z., BINLIN L. Spatiotemporal Dynamics and Decoupling Fertilizer-Driven Agricultural Non-Point Source Pollution in Southwest China. Polish Journal of Environmental Studies, **35** (2), 2123, **2026**.
5. WANG M., CHEN L., WU L., ZHANG L., XIE H., SHEN Z. Review of nonpoint source pollution models: Current status and future direction. Water, **14** (20), 3217, **2022**.
6. HUSSAIN F., AHMED S., MUHAMMAD ZAIGHAM ABBAS NAQVI S., AWAIS M., ZHANG Y., ZHANG H., RAGHAVAN V., ZANG Y., ZHAO G., HU J. Agricultural non-point source pollution: Comprehensive analysis of sources and assessment methods. Agriculture, **15** (5), 531, **2025**.
7. GUAN R., WU L., LI Y., MA B., LIU Y., ZHAO C., WANG Z., ZHAO Y. Evaluating the impacts of fertilization and rainfall on multi-form phosphorus losses from agricultural fields: A case study on the North China Plain. Agronomy, **14** (9), 1922, **2024**.
8. LU Y., WANG C., YANG R., SUN M., ZHANG L., ZHANG Y., LI X. Research on the progress of agricultural non-point source pollution management in China: A review. Sustainability, **15** (18), 13308, **2023**.
9. QIU W., ZHONG Z., LI Z. Agricultural non-point source pollution in China: Evaluation, convergence characteristics and spatial effects. Chinese Geographical Science, **31** (3), 571, **2021**.
10. TAN Q., SU H., ZHANG Y. Evolution characteristics and control suggestions for agricultural non-point source pollution in the Yellow River Basin of China. Water, **17** (11), 1626, **2025**.
11. WANG X., WU L., LUO Y., LIU Y., WANG R. Integrated export instream coefficient model for accurate nonpoint source pollution estimation and management in the Yellow River Basin. Scientific Reports, **15** (1), 26302, **2025**.
12. CHEN Y., MIAO J. What determines China's agricultural nonpoint source pollution? An improved logarithmic mean Divisia index decomposition analysis. Journal of Agricultural & Resource Economics, **48** (2), 237, **2023**.
13. YOU L., ROS G.H., CHEN Y., SHAO Q., YOUNG M.D., ZHANG F., DE VRIES W. Global mean nitrogen recovery efficiency in croplands can be enhanced by optimal nutrient, crop and soil management practices. Nature Communications, **14** (1), 5747, **2023**.
14. BAI Z., ZHANG X., XU J., LI C. Can farmland transfer reduce fertilizer nonpoint source pollution? Evidence from China. Land, **13** (6), 798, **2024**.
15. HUANG D., ZHU Y., YU Q. Spatial spillover effects of agricultural agglomeration on agricultural non-point source pollution in the Yangtze River Basin. Sustainability, **14** (24), 16390, **2022**.
16. DAGUM C. A new approach to the decomposition of the Gini income inequality ratio. Empirical Economics, **22** (4), 515, **1997**.
17. MORAN P.A.P. Notes on continuous stochastic phenomena. Biometrika, **37** (1-2), 17, **1950**.
18. ELHORST J.P. Applied spatial econometrics: Raising the bar. Spatial Economic Analysis, **5** (1), 9, **2010**.
19. YAN M., ZHAO J., QIAO J., HAN D., ZHU Q., YANG Y., LIU Q., WANG Z. Spatial pattern evolution and influencing factors on agricultural non-point source pollution in small town areas under the background of rapid industrialization. International Journal of Environmental Research and Public Health, **20** (3), 2667, **2023**.
20. HUA C., ZHANG J., LONG Z., WOODWARD R.T. Effects of policy for controlling agricultural non-point source pollution in China: From a perspective of regional and policy measures differences. International Journal of Environmental Research and Public Health, **20** (4), 3741, **2023**.
21. TAO Y., LIU J., GUAN X., CHEN H., REN X., WANG S., JI M. Estimation of potential agricultural non-point source pollution for Baiyangdian Basin, China, under different environment protection policies. PLoS ONE, **15** (9), e0239006, **2020**.
22. HE X., TIAN J., ZHANG Y., ZHAO Z., CAI Z., WANG Y. Attribution and driving force of nitrogen losses from the Taihu Lake Basin by the InVEST and GeoDetector models. Scientific Reports, **13** (1), 7440, **2023**.
23. LI X., XI B., HUANG L. Zoning management for agricultural non-point source pollution: a national-scale perspective in China. Emerging Contaminants and Environmental Health, **1** (1), 2, **2025**.
24. GAO M., LI F., HUAN M., ZHU R., ZHENG Z., HE K., ZHOU X., LI J. Long-term reduced agricultural nonpoint source pollution driven by rural population aging. Humanities and Social Sciences Communications, **12** (1), 553, **2025**.
25. XU L., JIANG J., LU M., DU J. Spatial-temporal evolution characteristics of agricultural intensive management and its influence on agricultural non-point source pollution in China. Sustainability, **15** (1), 371, **2023**.
26. XU B., NIU Y., ZHANG Y., CHEN Z., ZHANG L. China's agricultural non-point source pollution and green growth: interaction and spatial spillover. Environmental Science and Pollution Research, **29** (40), 60278, **2022**.
27. ZHANG F., WANG F., HAO R., WU L. Agricultural science and technology innovation, spatial spillover and

agricultural green development – taking 30 provinces in China as the research object. Applied Sciences, **12** (2), 845, **2022**.
28. GAO X., LI B., JIANG S., NIE Y. Can increasing scale efficiency curb agricultural nonpoint source pollution? International Journal of Environmental Research and Public Health, **18** (16), 8798, **2021**.
29. ZHANG W., GAO P., CHEN Z., QIU H. Preventing agricultural non-point source pollution in China: The effect of environmental regulation with digitization. International Journal of Environmental Research and Public Health, **20** (5), 4396, **2023**.
30. YE F., SUN S., RAZZAQ A., ZHANG Q. Harvesting environmental sustainability – the fertilizer use efficiency gains of China's high-standard farmland initiative. Humanities and Social Sciences Communications, **12** (1), 846, **2025**.
31. DA B., WU Y., BAO W. Analysis of spatial distribution and spillover effects of fertilizer application intensity in Inner Mongolia, China. Sustainability, **16** (11), 4697, **2024**.
32. LIANG F., LI G., ZHENG W.-L., SUN F., YANG Q. Can agricultural subsidy reform promote reduction of fertiliser nonpoint source pollution? Evidence from China. Agricultural Economics, **71** (9), 485, **2025**.
33. DRYGVAL P., DRYGVAL A., TABUNSHCHIK V. Assessment of organic carbon stocks at landscape levels using the InVEST software. Civil Engineering Journal. **11** (3), 1145, **2025**.